BRL

MEMORANDUM REPORT NO. 1258
April 1960

FREE FLIGHT RANGE TESTS OF A 10-CALIBER CONE CYLINDER

Eugene D. Boyer

Department of the Army Project No. 5B03-03-001
Ordnance Management Structure Code No. 5010.11.814

BALLISTIC RESEARCH LABORATORIES

ABERDEEN PROVING GROUND, MARYLAND

BALLISTIC RESEARCH LABORATORIES

MEMORANDUM REPORT NO. 1258

APRIL 1960

FREE FLIGHT RANGE TESTS OF A 10-CALIBER CONE CYLINDER

Eugene D. Boyer

Department of the Army Project No. 5B03-03-001
Ordnance Management Structure Code No. 5010.11.814
(Ordnance Research and Development Project No. TB3-0108)

ABERDEEN PROVING GROUND, MARYLAND

BALLISTIC RESEARCH LABORATORIES

MEMORANDUM REPORT NO. 1258

EDBoyer/amw
Aberdeen Proving Ground, Md.
April 1960

FREE FLIGHT RANGE TESTS OF A 10-CALIBER CONE CYLINDER

ABSTRACT

The aerodynamic properties of a ten-caliber cone cylinder are presented and analyzed. The Magnus data are definitely non-linear. It is shown that at subsonic Mach number the non-linear Magnus moment should cause a limit motion. Finally the data are combined with results of a finned model program to yield the properties of the fins.

TABLE OF CONTENTS

SYMBOLS

I_X	Axial moment of inertia (gm - in^2)
I_y	Transverse moment of inertia (gm - in^2)
cm	Center of mass (inches from base)
CP_n	Center of pressure of the normal force (calibers from base)
d	Diameter (in)
$K_{10,\ 20}$	Size of yaw arms at mid range (rad)
C_D	Drag Coefficient
$C_{D_{\delta^2}}$	Yaw drag coefficient (rad^{-2})
$C_{N_{p\alpha}}$	Magnus force coefficient
$C_{N_q} + C_{N_{\dot{\alpha}}}$	Damping force coefficient
$C_{M_q} + C_{M_{\dot{\alpha}}}$	Damping moment coefficient
C_{N_α}	Normal force coefficient
C_{M_α}	Overturning moment coefficient
$C_{M_{p\alpha}}$	Magnus moment coefficient
m	Mass (gm)
M	Mach number
n	Twist of rifling in calibers
	Number of yaw observations
N_T	Number of time of observations

s	Gyroscopic stability factor $= \frac{2A^2 v^2}{\rho d^5 B C_{M_\alpha} \pi}$
S_L	Size of swerve arm (in)
$\overline{\delta^2}$	Mean squared yaw (deg^2)
δ_e^2	Effective squared yaw, $K_{10}^2 + K_{20}^2 + \frac{K_{10}^2 \phi_1' - K_{20}^2 \phi_2'}{\phi_1' - \phi_2'}$ (rad^2)
ϵ_s	Error in swerve fit (in)
ϵ_y	Error in yaw fit (rad)
$\phi_{1,2}'$	Turning rates of yaw arms (deg/ft)
$\lambda_{1,2}$	Yaw damping rates (ft^{-1})
ρ	Relative air density
S	Reference area
ℓ	Reference length
$\cdot$	Indicates derivatives with respect to time.
$\sim$	Indicates quantities in non-rotating coordinate system
L,M,N	Aerodynamic moments about missile-fixed xyz axes, respectively
XYZ	Components of aerodynamic force along the missile-fixed x, y, z axes.
p,q,r	Components of the angular velocity of the missile in space along the x, y, z axes.
V	Magnitude of missile's velocity
α	Angle of attack (rad)
β	Angle of sideslip (rad)
γ	Cosine of angle between missile's axis and trajectory

$^{a}p_{\alpha}$

$^{b}p_{\alpha}$ } Defined by Eq. (3)

$^{c}p_{\alpha}$

INTRODUCTION

Over a period of years systematic investigations to determine the aerodynamic properties of a simple finned projectile have been carried out in the free flight ranges [1, 2, 3, 4, 5]. The model consisted of a ten-caliber long cone-cylinder body and four wedge-section fins at the base of the body. The rectangular planform fins extended one caliber out from the surface of the body and had a chord of one caliber.

As a part of the overall program it was decided to test the body alone in order to permit evaluation of aerodynamic effects of the fin assembly*. In order to test the body alone it was necessary to spin-stabilize** the model. A ten-caliber long projectile is close to the limit for stabilization by spin and considerable technical difficulties were encountered as a result of the high spin required. Tests at Mach numbers in excess of 1.5 were not possible.

The behavior of the body as a spin-stabilized projectile produced some interesting results in its own right and these are discussed in the first section of the results. The second section gives the net aerodynamic properties of the cruciform fin assembly by utilizing the previously determined data for the total configuration and subtracting from those data the new data for the body alone. In order to supply a reference frame the results are compared with linearized theory at the higher Mach numbers. A determination of the drag effects based on estimates of the body drag has been made previously. The use of the current data does not markedly change the results which are represented here for completeness.

---

* Currently there are ample wind tunnel data[6,7] on long bodies of revolution to permit the determination of fin effects by stripping the body effects from finned range model data. This program was fired in 1952 when there were little tunnel data. The data on Magnus and damping moments seems to be sufficiently interesting to warrant publication at this time.

** Spin sometimes produces noticeable changes in the aerodynamic coefficients, but the effects are probably negligible for the present purpose[8].

FIRING PROGRAM

Twelve 20-mm diameter models, six each of two center-of-mass positions were constructed to be fired at Mach 1.7 from a one-in-ten twist tube. Initial launchings resulted in structural failure. Hardness checks indicated that the strength of the aluminum used in the models was much below the design limits and that there was little chance of pursuing the original program with the remaining models. As a result the program's purpose was broadened to include subsonic data and seven successful models were launched at M = 0.8. Subsequent models were manufactured of more adequate aluminum and, although there was still difficulty in launching at M = 1.7, twelve models were fired successfully in the Aerodynamics Range[9] between M = 1.1 and 1.5. The physical properties of the models are given in Figure 1 and a photograph of the models in Figures 2A and 2B. The aerodynamic data[10] obtained from the range firings are given in Table I and the reduction and motion parameters in Table II.

RESULTS

Aerodynamic Properties and Stability of the Body

This extremely long model is difficult to stabilize gyroscopically, but by careful consideration of the inertial design it can be stabilized. Previous information[11] had also indicated that even a nine-caliber long model is difficult to stabilize dynamically.

The aerodynamic forces and moments are defined by the following expressions:

$$\text{Drag} = \frac{\rho V^2 S C_D}{2}$$

$$L = \frac{\rho V^2 S \ell C_{\ell p}}{2} \left(p\ell/V\right)$$

$$\tilde{Y} + i\tilde{Z} = -\frac{V^2 S \rho \ell}{2} \left\{ \left[C_{N_\alpha} + i \frac{p\ell}{V} C_{N_{p\alpha}} \right] \tilde{\xi} + i C_{N_q} \left[\frac{(q + i\gamma)\ell}{V} \right] + C_{N_{\dot{\alpha}}} \left(\frac{\dot{\tilde{\xi}} \ell}{V} \right) \right\}$$

$$\tilde{M} + i\tilde{N} = \frac{V^2 S \ell \rho}{2} \left\{ \left[(p\ell/V) C_{M_{p\alpha}} - i C_{M_\alpha} \right] \tilde{\xi} + C_{M_q} \left[\frac{(q + i\gamma)\ell}{V} \right] - i C_{M_{\dot{\alpha}}} \left(\frac{\dot{\tilde{\xi}} \ell}{V} \right) \right\}$$

Where $\tilde{\xi} = \tilde{\beta} + i\tilde{\alpha}$ (angles measured in non-spinning coordinates).

$S = \pi/4 \; d^2$

$\ell = d$

The aerodynamic properties are given in Figures 3 through 13.

NOTE: The above definitions of the aerodynamic coefficients differ in two ways from those defined in Reference 5: (1) The signs of C_N's have been reversed so that C_{N_α} will have its usual property of being positive; (2) the (1/2) factors which appeared in Reference 5 with the coefficients involving angular velocities have been omitted. A conversion table is given:

this report	Ref. 1, 5, 11
C_{N_α}	$-C_{N_\alpha}$
$C_{N_{p\alpha}}$	$-(1/2)\ C_{N_{p\alpha}}$
$C_{N_q} + C_{M_{\dot{\alpha}}}$	$-(1/2)\ (C_{N_q} + C_{N_{\dot{\alpha}}})$
C_{M_α}	C_{M_α}
$C_{M_{p\alpha}}$	$(1/2)\ C_{M_{p\alpha}}$
$C_{M_q} + C_{M_{\dot{\alpha}}}$	$1/2\ C_{M_q} + C_{M_{\dot{\alpha}}}$

In general the individual accuracy of the aerodynamic properties of a given model are on the order of:

Coefficient	Probable Error
C_D	0.5%
C_{M_α}	1%
C_{N_α}	5%
$C_{N_{p\alpha}}$	10%
$C_{M_q} + C_{M_{\dot{\alpha}}}$	10%

However in determining properties from combinations of the data and in correlating linear determined coefficients of non-linear properties the scatter can exceed the individual accuracy.

Drag Force Coefficient

The drag force coefficient, C_D, was obtained by fitting a cubic equation to the time-distance data for each round. These data were

then reduced to zero yaw by the relationship $C_D = C_{D_o} + C_{D_{\delta^2}} \delta^2$. For $M = 0.8$, $C_{D_{\delta^2}} = 5.88$ (radians)$^{-2}$. The scarcity of data at any one Mach number, in the supersonic region, prevented an accurate determination of $C_{D_{\delta^2}}$. At supersonic velocities, $C_{D_{\delta^2}}$ was estimated to be 11.2. The zero-yaw drag curve is given in Figure 3. A shadowgraph of the spin stabilized model at $M = 1.51$ is given in Figure 4a and a shadowgraph of the finned model at $M = 1.53$ is given in Figure 4b.

Overturning Moment and Normal Force

The overturning moment coefficient, C_{M_α}, is obtained from the frequencies of the fitted epicyclic yawing motion of the model. The values given in the table and Figure 5 are computed for each model's individual center of mass position.

The normal force coefficient, C_{N_α}, is given in Figure 6. The plotted points were obtained from the swerving motion and the curve is determined from the pitching and yawing motion of the two different center of mass models. The center of pressure is given in Figure 7.

Spin Deceleration, Magnus and Damping Properties

The spin deceleration moment coefficient, C_{ℓ_p}, given in Figure 8 was determined directly from the roll measurements of pins in the base of the models. The Magnus force, $C_{N_{p\alpha}}$, is also given in Figure 8. The points were determined from the swerving motion and the dashed curve from the center of mass method. The damping force coefficient, $C_{N_q} + C_{N_{\dot{\alpha}}}$ (at the centroid) is -22 subsonically and -45 supersonically.

The non-linear force and moment theory of Reference 12 was employed in the treatment of the Magnus and damping moment data. In this

reference, C. H. Murphy shows that if there is a quadratic dependence of $C_{M_{p\alpha}}$ on yaw, the epicyclic motion is affected in such a way that the usual linear formulas are replaced by the following combinations of coefficients:

Assuming $C_{M_{p\alpha}} = a_{p\alpha} + b_{p\alpha}\,\delta^2$

where $\delta^2 = |\tilde{\xi}|^2$

then $(C_{M_q} + C_{M_{\dot{\alpha}}})$ range $\doteq C_{M_q} + C_{M_{\dot{\alpha}}} - b_{p\alpha}\, I_Y/I_X \left(\frac{\phi_1' + \phi_2'}{\phi_1' - \phi_2'}\right)$ (1)

$(K_{10}^2 - K_{20}^2)$

$(C_{M_{p\alpha}})$ range $\doteq a_{p\alpha} + b_{p\alpha}\ \delta_c^2$ (2)

Range values of $C_{M_{p\alpha}}$ and $C_{M_q} + C_{M_{\dot{\alpha}}}$ were fitted to these equations and values of $C_{M_q} + C_{M_{\dot{\alpha}}}$, $a_{p\alpha}$ and $b_{p\alpha}$ were obtained. The value of $b_{p\alpha}$ was computed from equation (2). Subsonically, $b_{p\alpha}$ was determined to be + 250 (Fig. 9). The data from the supersonic models indicated a Mach number dependence of $a_{p\alpha}$ and the following expression was used to perform a least squares fit on the data.

$$C_{M_{p\alpha}} \text{ range} = a_{p\alpha} + b_{p\alpha}\ \delta_e^2 + c_{p\alpha}\,\Delta M \qquad (3)$$

$b_{p\alpha}$ was found to be + 340 at M = 1.3 and $c_{p\alpha}$ was 0.16. The Magnus moment coefficient at zero yaw is plotted in Figure 10. Values of $C_{N_{p\alpha}}$ are given for the individual rounds in Table II and Figure 8.

The linear value of $C_{M_{p\alpha}}$, namely $a_{p\alpha}$, is a quite large negative number at subsonic Mach number. According to the usual linear stability theory this Magnus moment will cause an undamping of pitching and yawing

motion. In order to evaluate the influence of the nonlinearity in the Magnus moment an amplitude plane[13] was constructed for Mach number equal to 0.8 (Figure 11). According to the analysis the motion should approach a limit epicyclic motion with amplitude about 5°. This type of limit motion has been observed in other spinning shell.[14]

While in theory Equation (1) can be treated to determine $b_{p\alpha}$ in a manner similar to that employed in Equation (2) in practice it frequently occurs that the relative size of the terms prevents a determination of $b_{p\alpha}$. In this case it is preferable to eliminate $b_{p\alpha}$ between Equations (1) and (2) and solve for $C_{M_q} + C_{M_{\dot{\alpha}}}$. This was done and the results given in Figure 10. The data indicate a strong trend toward positive values of $C_{M_q} + C_{M_{\dot{\alpha}}}$ in the transonic region.

Properties of the Cruciform Tail Assembly

The cruciform tail assembly consisted of four fins with wedge airfoil sections of 8 percent thickness. The fins had a square planform with a chord equal to the missile body diameter and the base of the fins were flush with the missile base. (See Figure 2B)

The range of validity of any computation of the aerodynamic effects of the tail section would be rather short since the test data extend to only M = 1.5. Since no specific test of a theory was envisioned only reference level computations were made. These utilized two-dimensional theory and tip effects but ignored any form of interference, since any reasonable allowance for these effects would have involved extensive computations which seemed unwarranted.[15]

The fin effects were determined by subtracting the data for the body-alone tests from the data for the complete configuration. In this process the mutual interference effects between the fins and body are retained and ascribed to the fins. These data furnish the net performance of the four fins situated at the base of the body. Applications of these results to even similar fins at a different body location or on a fundamentally

different body should only be made with caution. The fin properties are given as a function of Mach number in Figures 12 and 13. A reference area of $\pi d^2/4$, and a reference length, d, are used to determine the coefficients.

DRAG

The drag force coefficient is fairly constant at velocities greater than M = 1.25 and increases rapidly as the Mach number decreases toward sonic speeds. The fin assembly yields about 40% of the total drag of the missile subsonically and about 30% supersonically. It should be noted that previous data[3] show the drag contributions to be very sensitive to fin position on the body.

Roll Damping

The roll damping parameters of the body, as might be expected, are so much less than those of the fins (about 3 percent) that to within the usual needs of accuracy they can be ignored. The use of any convenient scales leaves the data of Reference 2 visibly unaltered.

Normal Force and Center of Pressure

The normal force coefficient variation supersonically is of the same shape as predicted by theory; however, the predicted value is about 40 percent low. The observed center of pressure agrees with the predicted values.

Damping Moment

The predicted damping moment is 10 percent less than the observed values.

Eugene D. Boyer

EUGENE D. BOYER

REFERENCES

1. MacAllister, L. C. The Aerodynamic Properties of a Simple Non-Rolling Finned Cone-Cylinder Configuration Between Mach Numbers 1.0 and 2.5, BRL Report 934, May 1955.

2. Bolz, R. F., Nicolaides, J. D. A Method of Determining Some Aerodynamic Coefficients from Supersonic Free Flight Tests of a Rolling Missile, Journal of the Aeronautical Sciences, Vol. 17, p. 609, October 1950.

3. MacAllister, L. C., Roschn, E. J. The Drag Properties of Several Winged and Finned Cone-Cylinder Models, BRIM 849, October 1954.

4. Nicolaides, J. D., Bolz, R. A. On The Pure Rolling Motion of Winged and/or Finned Missiles in Varying Supersonic Flight, Journal of the Aeronautical Sciences, Vol. 20, p. 160, March 1952, also published as BRL Report 799, March 1952.

5. Nicolaides, J. D., MacAllister, L C. A Review of Aeroballistic Range Research on Winged and/or Finned Missiles, Bureau of Ordnance TN 5, 1955.

6. Buford, W. E., Shatuwoff, S. The Effects of Fineness Ratio and Mach Number on the Normal Force and Center of Pressure of Conical and Ogival Head Bodies, BRLM 760 (C), February 1954.

7. Jaeger, B. F. A Review of Experiment and Theory Applicable to Cone-Cylinder and Ogive-Cylinder Bodies of Revolution in Supersonic Flow, NAVORD-5239, June 1956.

8. Murphy, C. H., Schmidt, L. E. Effect of Spin on Aerodynamic Properties of Bodies of Revolution, BRIM 715, August 1953.

9. Braun, W. F. The Free Flight Aerodynamics Range, BRL Report 1048, July 1958.

10. Murphy, C. H. Data Reduction for the Free Flight Spark Ranges, BRL Report 900, February 1954.

11. Murphy, C. H., Schmidt, L E. The Effect of Length on the Aerodynamic Characteristics of Bodies of Revolution in Supersonic Flight, BRL Report 876, August 1953.

12. Murphy, C. H. The Measurement of Non-Linear Forces and Moments by Means of Free Flight Tests, BRL Report 974, February 1956.

13. Murphy, C. H. Prediction of the Motion of Missiles Acted on by Non-Linear Forces and Moments, BRL Report 995, October 1956.

14. Roecker, E. T. The Aerodynamic Properties of the 105mm HE Shell, M1, In Subsonic and Transonic Flight, BRLM 929, September 1955.

15. Bonney, E. A. Aerodynamic Characteristics of Rectangular Wings at Supersonic Speeds, Journal of the Aeronautical Sciences, February 1947.

TABLE I

Aerodynamic Coefficients

Center of Mass at 3.252 Calibers from Base

RD	M	$\sqrt{\delta^2}$ (deg)	C_D	C_{M_α}	C_{N_α}	$C_{M_q}+C_{M_{\dot\alpha}}$	$C_{M_{p\alpha}}$	C_{ℓ_p}	$C_{N_{p\alpha}}$
3921	.811	4.4	.323	9.12	+2.72	-19.6	- .46	-.0316	-1.1
3920	.818	2.1	.297	9.37	+2.44	-17.9	-1.22	-.0318	- .7
3919	.822	.7	.291	9.40	-	-	-	-.0323	-
3918	.868	2.8	.332	9.28	+2.65	-13.8	-1.20	-.0321	- .7
4623	1.151	2.1	.499	9.99	+2.72	-	-	-	-
4621	1.185	2.9	.513	10.27	+2.80	-32.0	- .51	-.0278	- .9
4636	1.331	2.1	-	10.64	+2.98	-	- .36	-	-
4634	1.409	1.6	.447	11.00	+2.75	-27.8	- .05	-.0257	-

Center of Mass at 3.752 Calibers from Base

3923	.808	3.2	.308	7.72	+2.62	-32.2	- .21	-	-1.0
3924	.812	1.8	.292	8.11	+2.47	-36.4	- .82	-	-
3922	.837	2.9	.314	7.89	+2.55	-22.3	- .61	-.0318	-1.0
4624	1.200	1.1	-	8.61	+2.67	-40.5	- .18	-	- .9
4627	1.214	2.4	.497	9.02	+2.78	-39.3	- .58	-.0275	- .9
4625	1.259	1.2	-	9.00	-	-44.5	- .36	-	- .8
4632	1.299	1.7	.485	9.23	+2.90	-41.1	- .16	-	-1.1
4638	1.356	1.6	.470	9.36	+2.80	-36.8	- .16	-.0280	-1.2
4637	1.363	1.0	.458	9.40	+2.62	-40.3	-	-	-
4628	1.452	1.3	.434	9.82	+2.78	-38.1	- .08	-.0255	-
4629	1.514	2.5	.433	9.63	+2.88	-46.9	- .61	-.0244	- .9

TABLE II

Reduction and Motion Parameters

RD	$\lambda_1 \times 10^3$	$\lambda_2 \times 10^3$	K_1 (RAD)	K_2 (RAD)	ϕ_1^1 (Deg/ft)	ϕ_2^1 (Deg/ft)	N	N_T	S_L (in)	s	$\delta_e^2 \times 10^2$ $(RAD)^2$
3921	1.92	- .47	.046	.060	13.22	1.61	21	7	.53	2.59	.763
3920	3.59	-2.26	.013	.033	13.19	1.67	26	9	.23	2.50	.129
3919	-	-	.011	.005	13.08	1.70	26	9	.06	2.46	-
3918	3.31	-2.13	.022	.040	13.23	1.66	26	8	.36	2.52	.241
4623	-	-	.010	.035	12.80	1.88	16	7	.22	2.24	.123
4621	3.02	- .81	.027	.040	12.72	1.97	21	9	.24	2.15	.316
4636	-	-	.022	.029	12.42	2.06	14	4	.17	1.87	.174
4334	1.63	.35	.024	.015	12.47	2.12	22	9	.08	2.02	.144
3923	2.38	- .01	.035	.042	16.90	1.34	16	6	.50	3.68	.417
3924	3.91	-1.33	.017	.026	16.82	1.41	20	6	.25	3.51	.122
3922	2.57	- .81	.028	.042	16.93	1.36	24	9	.48	3.62	.325
4624	3.06	.07	.027	.030	16.64	1.57	12	4	.25	3.17	.234
4627	3.43	- .48	.027	.029	16.74	1.74	22	8	.23	3.08	.229
4625	3.78	- .53	.016	.013	16.71	1.75	14	4	.09	3.06	.069
4632	3.09	.05	.017	.023	16.65	1.69	21	8	.19	2.98	.108
4638	2.74	.05	.019	.020	16.77	1.69	21	9	.15	3.01	.112
4637	2.26	.74	.013	.011	16.66	1.72	22	9	.08	2.95	.047
4628	2.35	.53	.011	.020	16.35	1.83	17	7	.13	2.77	.061
4629	1.71	1.74	.028	.031	16.61	1.76	21	9	.23	2.89	.251

PHYSICAL PROPERTIES

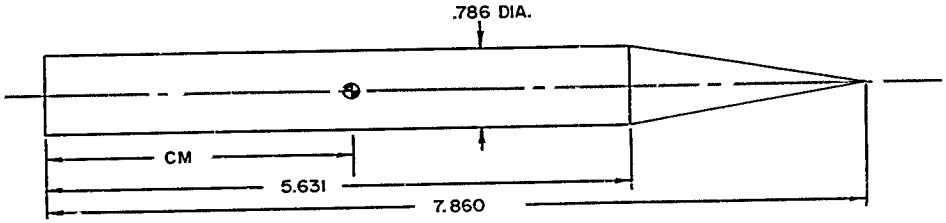

	FCM	RCM
A= GMS IN²	19.48	19.49
B= GMS IN²	585.66	735 67
CM= INS	2.949	2.557
WT. = GMS	241.91	227.93

FIG. 1

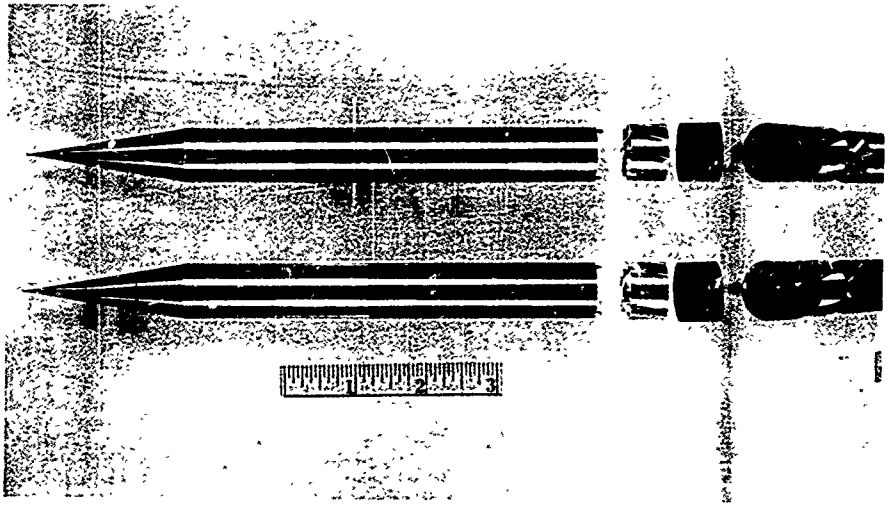

Fig. 2A - 10-Caliber Cone-Cylinder

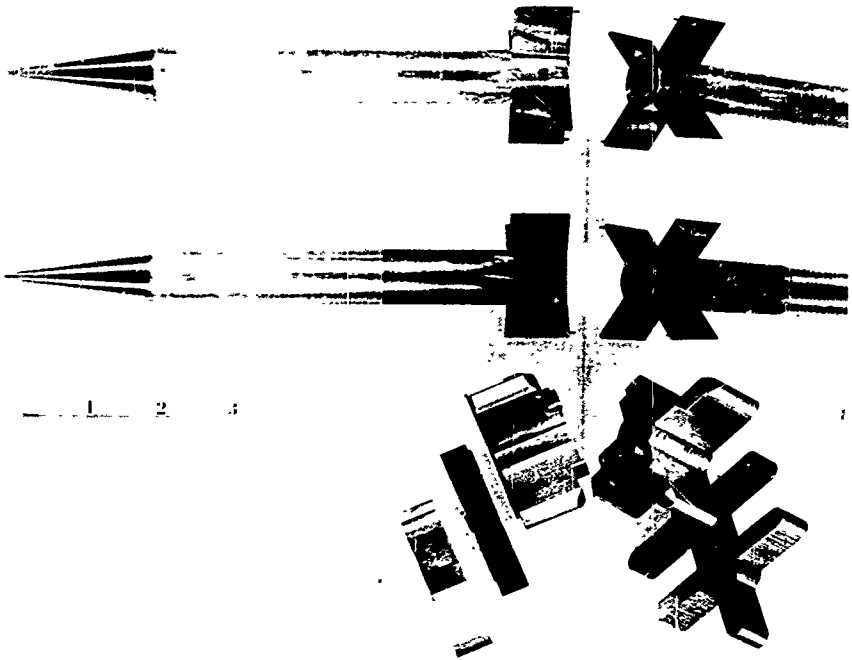

Fig. 2B - Finned Model

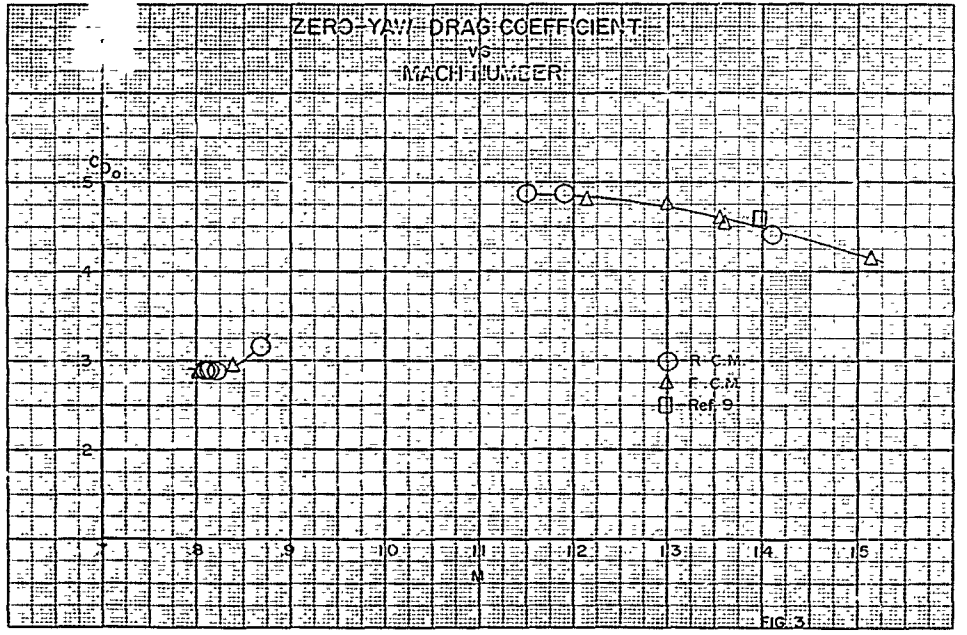
ZERO-YAW DRAG COEFFICIENT
VS
MACH NUMBER
C_{D_o}
.5
.4
.3
.2
.8
.9
1.0
1.1
1.2
1.3
1.4
1.5
M
R.C.M.
F.C.M.
Ref. 9

FIG. 3

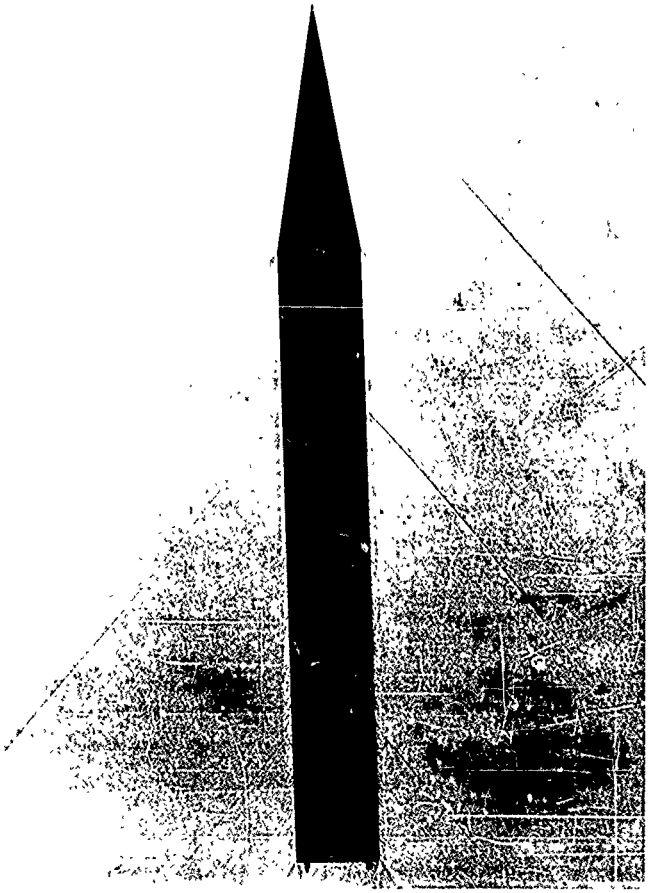

Fig. 4A - Rd. 4629, M = 1.51

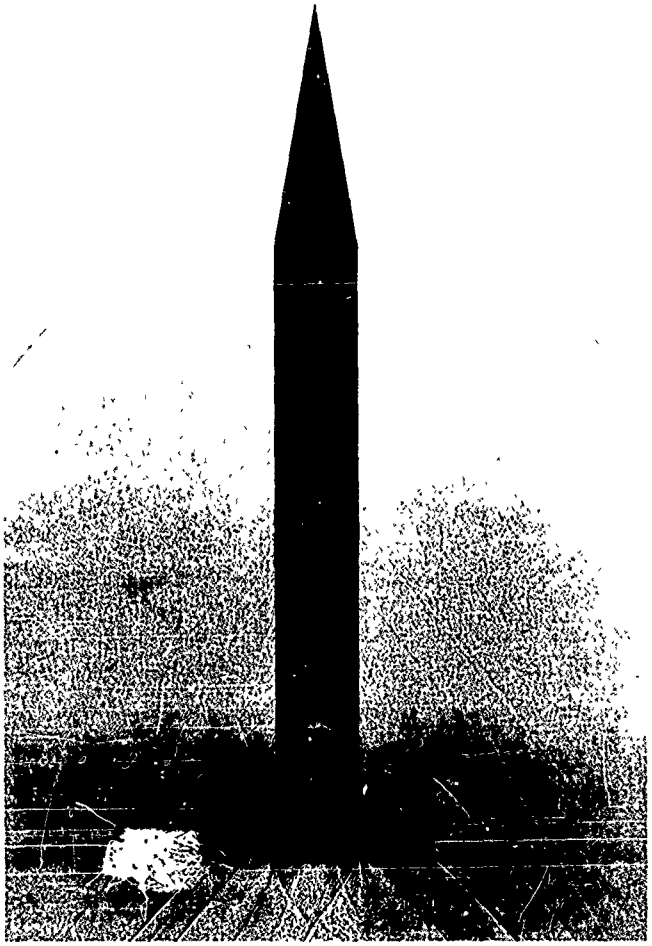

Fig. 4B - Finned Model, M = 1.53

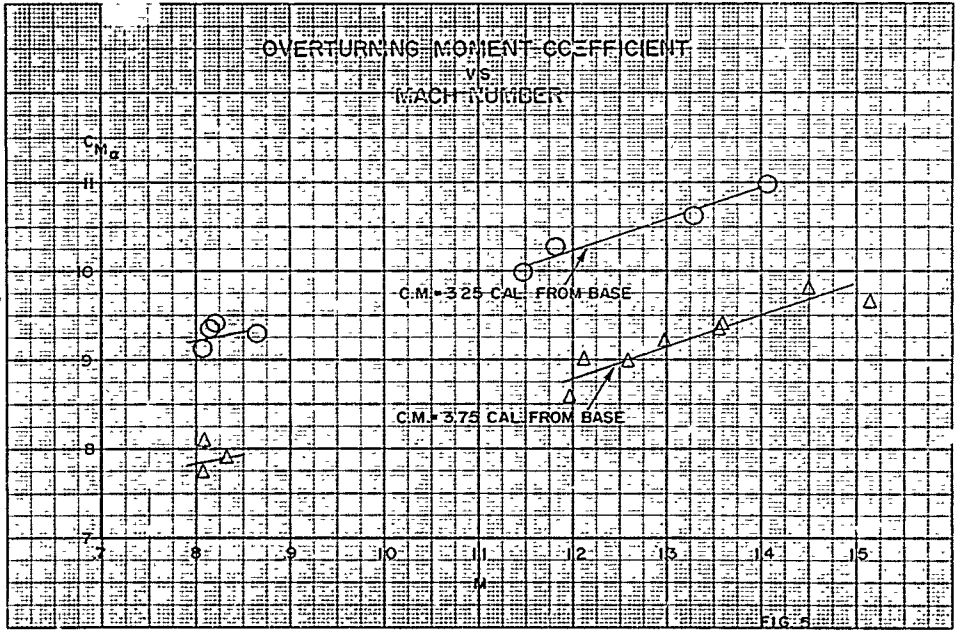
OVERTURNING MOMENT COEFFICIENT
VS
MACH NUMBER
C_{M_α}
11
10
9
8
7
C.M.= 3.25 CAL. FROM BASE
C.M.= 3.75 CAL. FROM BASE
7
8
9
10
11
12
13
14
15
M
12

FIG. 5

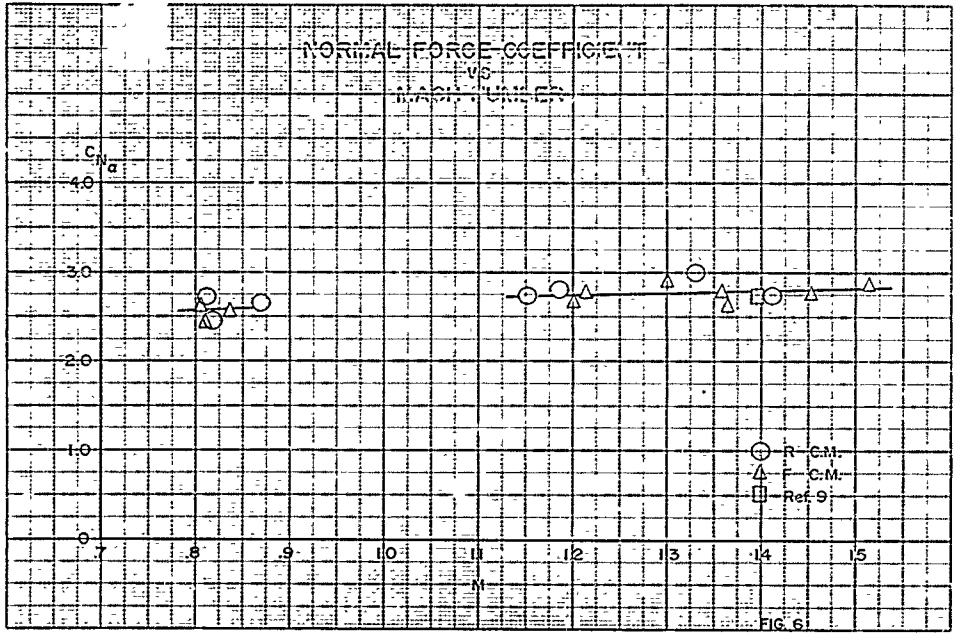
NORMAL FORCE COEFFICIENT
VS
MACH NUMBER
C_{N_α}
4.0
3.0
2.0
1.0
0
.7
.8
.9
1.0
1.1
1.2
1.3
1.4
1.5
M
R C.M.
F C.M.
Ref. 9

FIG. 6

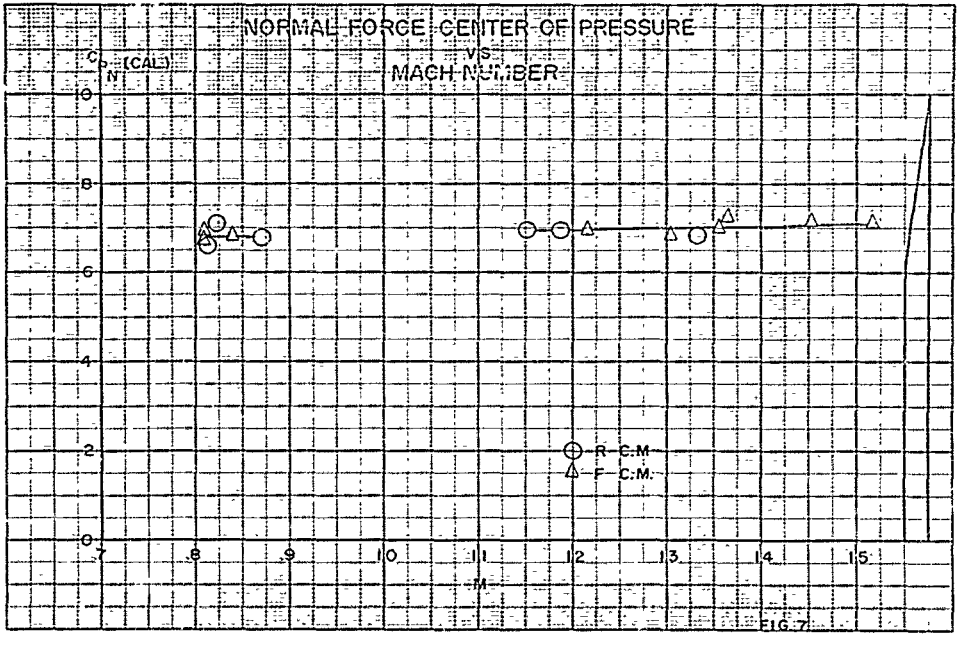
NORMAL FORCE CENTER OF PRESSURE
VS
MACH NUMBER
C_{p_N} (CAL)
10
8
6
4
2
0
.7
.8
.9
1.0
1.1
1.2
1.3
1.4
1.5
M
R C.M
F C.M.

FIG. 7

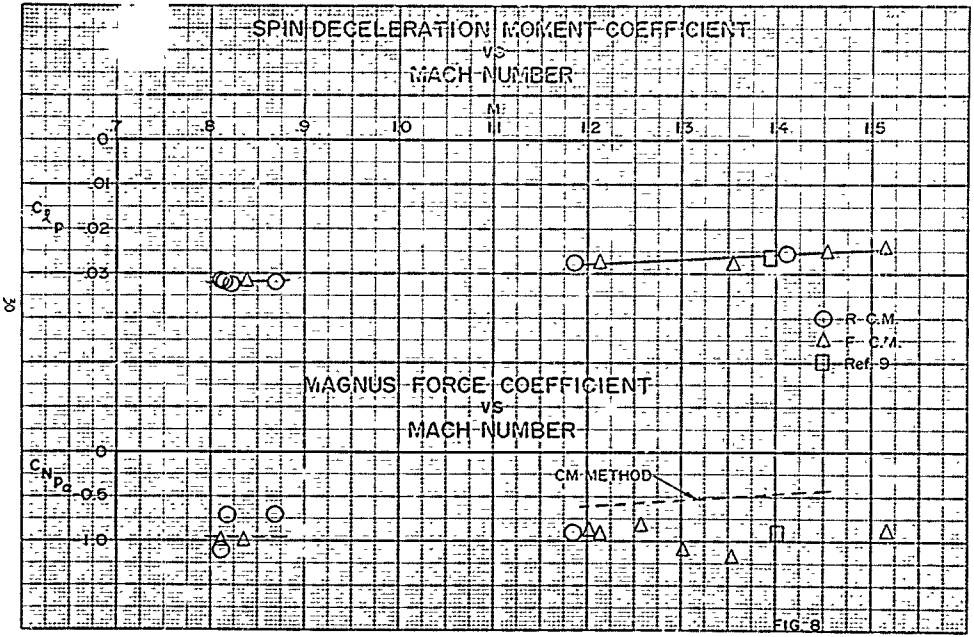
SPIN DECELERATION MOMENT COEFFICIENT
VS
MACH NUMBER
M
.7
.8
.9
1.0
1.1
1.2
1.3
1.4
1.5
0
-.01
-.02
-.03
C_{ℓ_p}
R-C.M.
F-C.M.
Ref. 9
MAGNUS FORCE COEFFICIENT
VS
MACH NUMBER
0
0.5
1.0
$C_{N_{P_\alpha}}$
CM METHOD

FIG. 8

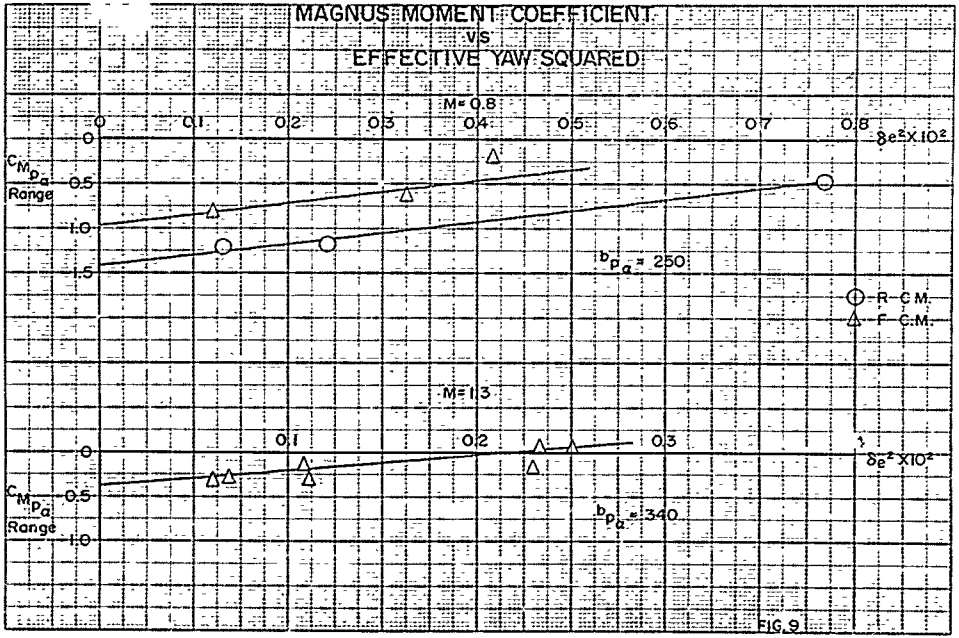
MAGNUS MOMENT COEFFICIENT
VS
EFFECTIVE YAW SQUARED
M= 0.8
0
0.1
0.2
0.3
0.4
0.5
0.6
0.7
0.8
$\delta_e^2 X 10^2$
$C_{M_{p_a}}$
Range
0
0.5
1.0
1.5
$b_{p_a} = 250$
R-C.M.
F-C.M.
M=1.3
0
0.1
0.2
0.3
$\delta_e^2 X 10^2$
$C_{M_{p_a}}$
Range
0.5
1.0
$b_{p_a} = 340$

FIG. 9

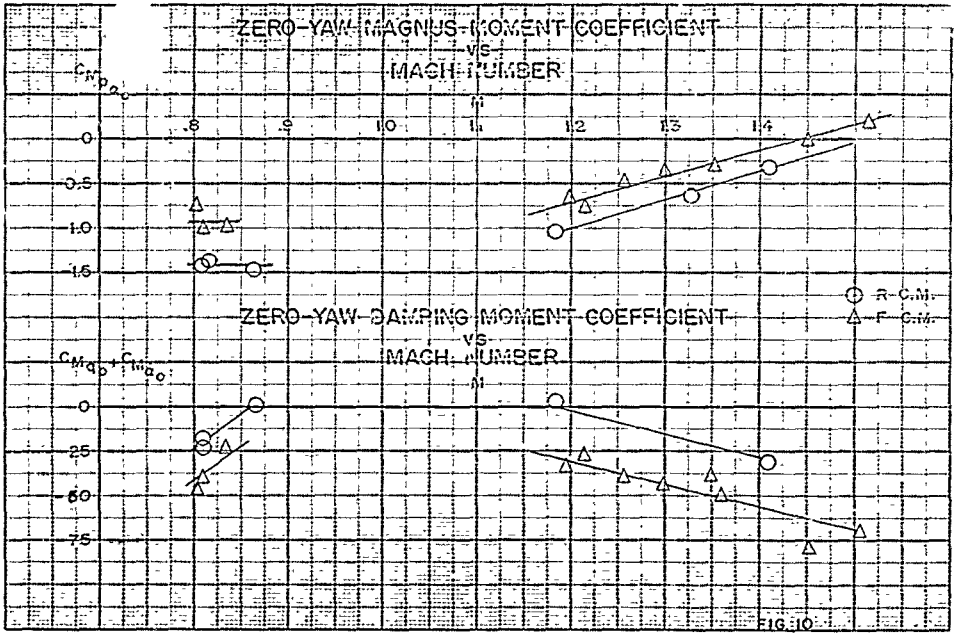
ZERO-YAW MAGNUS MOMENT COEFFICIENT
VS
MACH NUMBER
$C_{N_{p_{\alpha_0}}}$
0
-0.5
-1.0
-1.5
.8
.9
1.0
1.1
1.2
1.3
1.4
M
R. C.M.
F. C.M.
ZERO-YAW DAMPING MOMENT COEFFICIENT
VS
MACH NUMBER
$C_{M_{q_0}} + C_{M_{\dot{\alpha}_0}}$
0
-25
-50
-75
M

FIG. 10

AMPLITUDE PLANE

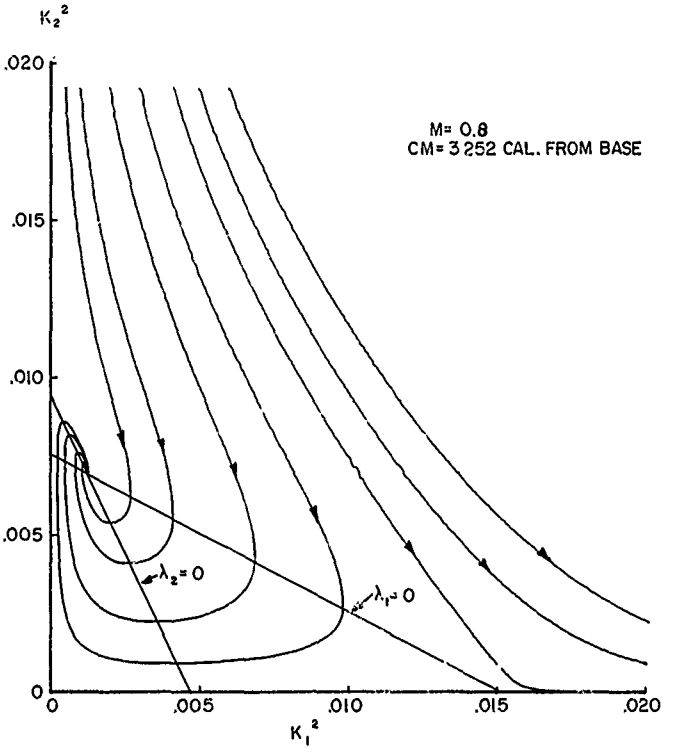

FIG. 11

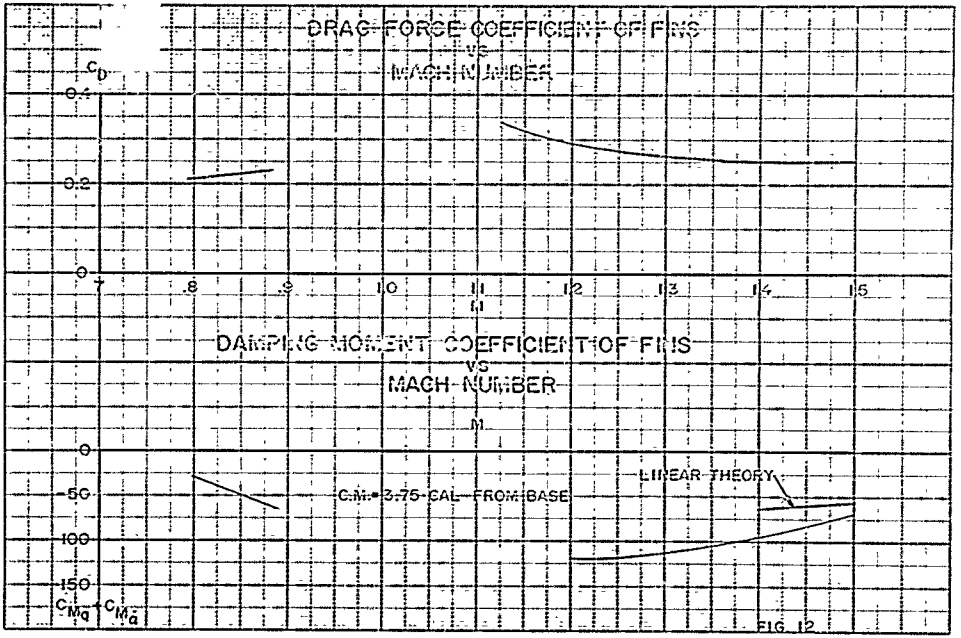
DRAG FORCE COEFFICIENT OF FINS
VS
MACH NUMBER
C_D
0.4
0.2
0
.7
.8
.9
1.0
1.1
1.2
1.3
1.4
1.5
M
DAMPING MOMENT COEFFICIENT OF FINS
VS
MACH NUMBER
M
0
-50
-100
-150
$C_{Mq} + C_{M\dot{\alpha}}$
C.M. = 3.75 CAL FROM BASE
LINEAR THEORY

FIG 12

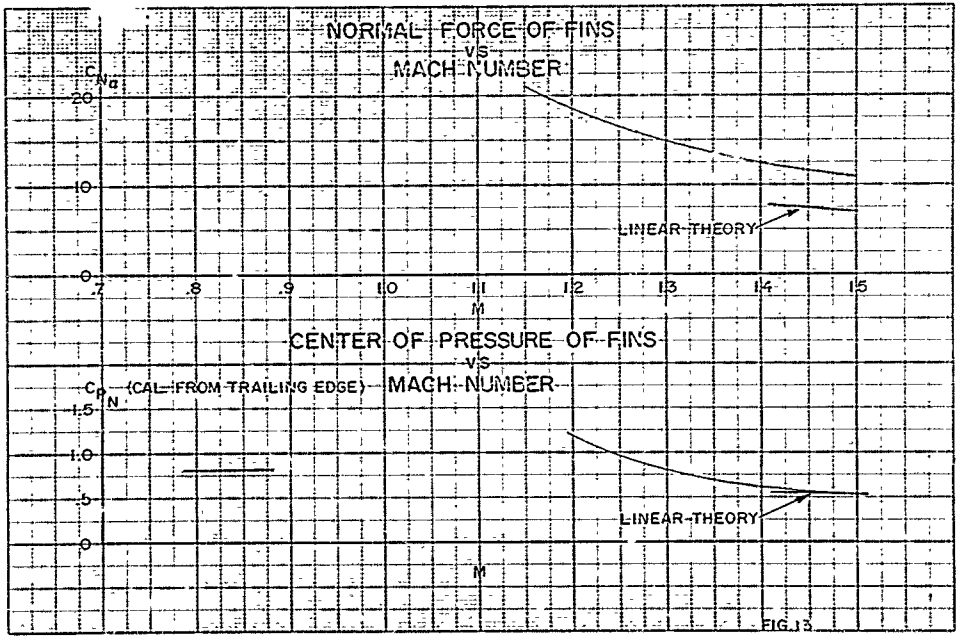
NORMAL FORCE OF FINS
VS
MACH NUMBER
C_{N_α}
20
10
0
LINEAR THEORY
.7
.8
.9
1.0
1.1
1.2
1.3
1.4
1.5
M
CENTER OF PRESSURE OF FINS
VS
C_{P_N} (CAL. FROM TRAILING EDGE) MACH NUMBER
1.5
1.0
.5
0
LINEAR THEORY
M

FIG. 13